Three-dimensional optical-transfer-function analysis of fiber-optical two-photon fluorescence microscopy

Min Gu and Damian Bird

Centre for Micro-Photonics, School of Biophysical Sciences and Electrical Engineering, Swinburne University of Technology, P.O. Box 218, Hawthorn 3122, Victoria, Australia

Received June 20, 2002; revised manuscript received October 30, 2002; accepted December 6, 2002

The three-dimensional optical transfer function is derived for analyzing the imaging performance in fiber-optical two-photon fluorescence microscopy. Two types of fiber-optical geometry are considered: The first involves a single-mode fiber for delivering a laser beam for illumination, and the second is based on the use of a single-mode fiber coupler for both illumination delivery and signal collection. It is found that in the former case the transverse and axial cutoff spatial frequencies of the three-dimensional optical transfer function are the same as those in conventional two-photon fluorescence microscopy without the use of a pinhole. However, the transverse and axial cutoff spatial frequencies in the latter case are 1.7 times as large as those in the former case. Accordingly, this feature leads to an enhanced optical sectioning effect when a fiber coupler is used, which is consistent with our recent experimental observation.

OCIS codes: 110.2350, 110.2990, 110.4850.

1. INTRODUCTION

The introduction of optical fibers into a scanning optical microscope for illumination source and signal collection isolates the vibration from lasers and electronic devices.[1–3] It also permits the system to be operated in novel imaging modes such as confocal microscopy,[1–4] differential interference microscopy,[5] interference microscopy,[6,7] double-pass microscopy,[8] single-photon fluorescence microscopy,[9] and two-photon fluorescence microscopy.[10–12] Among these, two-photon fluorescence microscopy based on an optical fiber coupler[12] is a promising tool for endoscopic imaging because of the feature of deep penetration associated with two-photon excitation[13] and the compactness of the system. In addition, a two-photon fluorescence microscope based on a fiber coupler exhibits higher axial resolution than microscopes using a large-area detector.[12,14]

To understand the imaging performance in fiber-optical scanning microscopy, one can introduce the concept of the three-dimensional (3-D) transfer function.[15] For a nonfluorescent sample, fiber-optical scanning microscopy behaves fully coherently, even for finite values of fiber spot size.[1,3,15] Therefore a 3-D coherent transfer function (CTF) has been developed for nonfluorescence imaging. It has been found that the utilization of optical fibers does not affect the passband of spatial frequencies but reduces the strength of the CTF, in particular along the axial direction.[16] However, this coherent nature is destroyed when a sample becomes fluorescent. An optical transfer function (OTF) has been developed for fiber-optical single-photon fluorescence microscopy.[17] It has been shown that using a fiber for signal collection removes negative tails and the missing cone of spatial frequencies of the 3-D OTF, both of which occur in confocal fluorescence microscopy with a finite-sized detector.[18–20] The aim of this paper is to develop an OTF analysis for fiber-optical two-photon fluorescence microscopy and thus to compare its imaging performance with that of conventional two-photon fluorescence microscopy consisting of a large-area detector.[14]

The paper is organized as follows. In Section 2 a mathematical expression for the 3-D OTF for fiber-optical two-photon fluorescence microscopy is derived. The relevant discussion regarding this expression is given in Section 3. Numerical calculations of the 3-D OTF for two types of fiber-optical two-photon fluorescence microscopy are described in Section 4. In particular, the effect of the fiber spot size on the 3-D OTF is investigated numerically. Finally, a conclusion is given in Section 5.

2. THREE-DIMENSIONAL OPTICAL TRANSFER FUNCTION

The schematic diagram of a fiber-optical two-photon fluorescence microscope is the same as Fig. 1 of Ref. 17. Without loss of generality, two lengths of fibers are considered for illumination and collection, respectively, so that the effect of optical fibers on illumination and collection can be investigated separately. The illumination beam of wavelength λ_1 from an optical fiber F_1 is focused by an objective P_1 onto a thick object. The two-photon excited fluorescence of wavelength λ_2 is then refocused, by a beam splitter and another lens P_2 acting as a collector, onto the tip of the second fiber F_2, which delivers the signal to a large-area detector D.

Although an ultrashort-pulsed laser beam is usually employed in order to obtain efficient two-photon excitation,[10,12,13] previous investigations[15,21] have demonstrated that the 3-D OTF under pulsed-beam illumination with a pulse width longer than 10 fs is not affected com-

pared with that under continuous-wave (cw) illumination. Accordingly, cw illumination is assumed throughout this paper.

Both single-photon and two-photon fluorescence processes are incoherent, and the difference between them is that the strength of two-photon fluorescence emission is proportional to the square of the excitation intensity while the strength of single-photon fluorescence emission is proportional to the excitation intensity. According to the analysis of fiber-optical single-photon fluorescence microscopy,[15,17] the image intensity from a scan point $\mathbf{r}_s$ in the fiber-optical two-photon fluorescence microscope can be expressed, in the given coordinate systems,[15,17] as

$$I(\mathbf{r}_s) = \int_{-\infty}^{\infty}\left\{\left|\int_{-\infty}^{\infty} f_1(x_0, y_0)\delta(z_0)\exp[ik(z_0 - z_1)] \times h_1(\mathbf{r}_0 + \mathbf{M}_1\mathbf{r}_1)\mathrm{d}\mathbf{r}_0\right|^4 o_f(\mathbf{r}_s - \mathbf{r}_1)\left|\int_{-\infty}^{\infty} f_2^*(x_2, y_2) \times \delta(z_2)\exp[ik(\pm z_1 - z_2)]h_2(\mathbf{r}_1 + \mathbf{M}_2\mathbf{r}_2)\mathrm{d}\mathbf{r}_2\right|^2\right\}\mathrm{d}\mathbf{r}_1, \quad (1)$$

where the fourth power of the first absolute value results from the quadratic dependence under two-photon excitation. $o_f(\mathbf{r})$ is the object function representing the fluorescence strength of the object under two-photon excitation. $f_1(x, y)$ and $f_2(x, y)$ are the amplitude profiles on the output end of fiber F_1 and on the input end of fiber F_2, respectively. $\mathbf{r}_0 = (x_0, y_0, z_0)$, $\mathbf{r}_1 = (x_1, y_1, z_1)$, and $\mathbf{r}_2 = (x_2, y_2, z_2)$ represent the positions in the illumination, object, and collection spaces, respectively. $\mathbf{M}_1$ and $\mathbf{M}_2$ are the demagnification matrices of the objective and the collector lenses, respectively.[15] Here $h_1(\mathbf{r})$ and $h_2(\mathbf{r})$ are the 3-D amplitude point-spread functions for the objective and collector lenses and are given by

$$h_j(x, y, z) = \int\int_{-\infty}^{\infty} P_j(\xi, \eta, z) \times \exp\left[\frac{i2\pi}{d_j\lambda_j}(\xi x + \eta y)\right]\mathrm{d}\xi\mathrm{d}\eta, \quad (2)$$

where $P_j(\xi, \eta, z)$ is the defocused pupil function of a lens[15,22] and j is an integer such that $j = 1, 2$.

Therefore the 3-D effective intensity point-spread function for fiber-optical two-photon fluorescence microscopy can be written as

$$h_i(\mathbf{r}) = |f_1(\mathbf{M}_1x, \mathbf{M}_1y) \otimes_2 h_1(\mathbf{M}_1\mathbf{r})|^4 \times |f_2^*(\mathbf{M}_1x, \mathbf{M}_1y) \otimes_2 h_2(\mathbf{r})|^2, \quad (3)$$

where $\otimes_2$ denotes the two-dimensional (2-D) convolution operation.

It was pointed out in previous studies[15,23] that an incoherent imaging system can be analyzed in terms of the 3-D OTF that is given by the 3-D Fourier transform of the effective intensity point-spread function. An OTF gives the transmission efficiency of each spatial-frequency component of the object through an imaging system. The fiber-optical two-photon fluorescence microscope can thus be described by the 3-D OTF $C(\mathbf{m})$, given by

$$C(\mathbf{m}) = C_1(\mathbf{m}) \otimes_3 C_2(\mathbf{m}), \quad (4)$$

where

$$C_1(\mathbf{m}) = \mathbf{F}_3\{|f_1(\mathbf{M}_1x, \mathbf{M}_1y) \otimes_2 h_1(\mathbf{M}_1\mathbf{r})|^4\}, \quad (5)$$

$$C_2(\mathbf{m}) = \mathbf{F}_3\{|f_2^*(\mathbf{M}_1x, \mathbf{M}_1y) \otimes_2 h_2(\mathbf{r})|^2\}. \quad (6)$$

Here $\mathbf{F}_3$ is the 3-D Fourier transform with respect to $\mathbf{r}_s$, and $\mathbf{m}$ represents the spatial-frequency vector with two transverse components m and n and one axial component s. Compared with Eq. (8) of Ref. 17, Eq. (5) is the 3-D OTF for a fiber-optical single-photon fluorescence microscope with identical illumination and collection fibers and equal illumination and fluorescence wavelengths. Thus Eq. (5) can be rewritten as an autoconvolution operation:

$$C_1(\mathbf{m}) = C_1'(\mathbf{m}) \otimes_3 C_1'(\mathbf{m}), \quad (7)$$

where

$$C_1'(\mathbf{m}) = \mathbf{F}_3\{|f_1(\mathbf{M}_1x, \mathbf{M}_1y) \otimes_2 h_1(\mathbf{M}_1\mathbf{r})|^2\}. \quad (8)$$

Suppose that both illumination and collection fibers are single-mode fibers of mode spot radii a_1 and a_2, respectively, and that the Gaussian approximation[24] holds for circularly polarized fibers. Further assume that the paraxial approximation[15] is used and that the objective and collector lenses, P_1 and P_2, are of identical circular aperture of radius a. Therefore the analytical expressions for $C(\mathbf{m})$, $C_1'(\mathbf{m})$, and $C_2(\mathbf{m})$ can be derived, in a cylindrical coordinate system as used previously,[15,17] as

$$C(l, s) = [C_1(l, s) \otimes_3 C_1(l, s)] \otimes_3 C_2(l, s), \quad (9)$$

$$C_1'(l, s) = \frac{\sqrt{\pi}\exp\{-A_1[(\beta^2l^2)/4 + (s/l)^2]\}}{\sqrt{A_1}\beta l} \times \mathrm{erf}\left(\sqrt{A_1}\,\mathrm{Re}\left\{\left[1 - \left(\frac{|s|}{l} + \frac{\beta l}{2}\right)^2\right]^{1/2}\right\}\right), \quad (10)$$

$$C_2(l, s) = \frac{\sqrt{\pi}\exp\{-A_2[l^2/4 + (s/l)^2]\}}{\sqrt{A_2}l} \times \mathrm{erf}\left(\sqrt{A_2}\,\mathrm{Re}\left\{\left[1 - \left(\frac{|s|}{l} + \frac{l}{2}\right)^2\right]^{1/2}\right\}\right), \quad (11)$$

where

$$A_j = \left(\frac{2\pi a a_j}{\lambda_j d_1}\right)^2, \qquad j = 1, 2, \quad (12)$$

is the normalized fiber spot size for illumination and collection fibers d_1 is the distance between the fiber and the lens P_j. Here the variables l and s are the radial and axial spatial frequencies normalized by $\sin(\alpha)/\lambda_2$ and $4\sin^2(\alpha/2)/\lambda_2$, respectively, where $\sin(\alpha)$ is the numerical aperture of the objective lens. β in Eq. (10) is the wave-

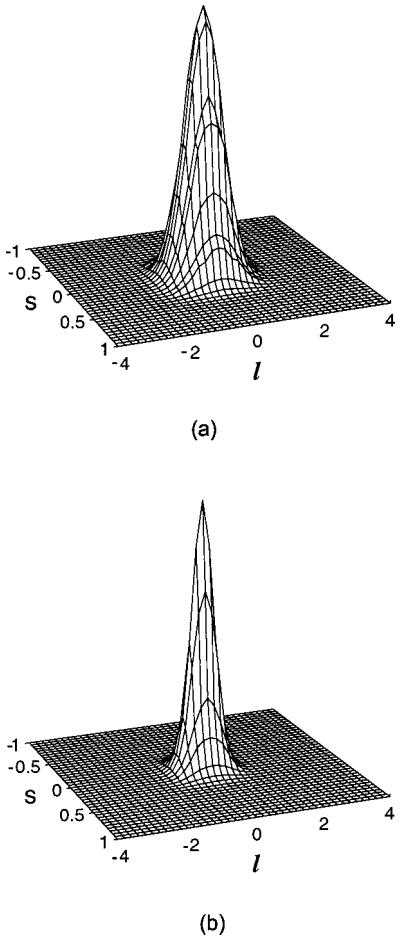

Fig. 1. 3-D OTF for fiber-optical two-photon fluorescence microscopy with a large-area detector: (a) $A_1 = 1$ and $A_2 \rightarrow \infty$, (b) $A_1 = 10$ and $A_2 \rightarrow \infty$.

length ratio of λ_1 to λ_2. Re{} denotes the real part of its argument, which becomes zero for negative values of the argument.

The function erf in Eqs. (10) and (11) is defined as

$$\mathrm{erf}(x) = \frac{2}{\sqrt{\pi}} \int_0^x \exp(-r^2)\mathrm{d}t, \tag{13}$$

which is called the error function.[25]

3. DISCUSSION

The significance of A_j is that it represents the ratio squared of the numerical aperture of the objective (collector) lens P_j to the numerical aperture of the illumination (collection) fiber.[15] An increase in the fiber spot size results from a decrease in the fiber numerical aperture.[24] Another way to vary the value of A_j for a given imaging system is to change the illumination wavelength.

With the help of Eqs. (9)–(13), the effect of these two parameters on the 3-D OTF for fiber-optical two-photon fluorescence microscopy can be evaluated. When $A_j \rightarrow 0$, the 3-D OTF in Eq. (9) becomes identical to that for two-photon fluorescence microscopy with a point source and a point detector.[14] If $A_j \rightarrow \infty$, it becomes zero, except for $l = s = 0$. In general, the 3-D OTF in Eq. (9) always has positive values because the fiber mode has been assumed to be a Gaussian function, which gives a positive Fourier spectrum. In this respect, this feature is different from that in two-photon fluorescence scanning microscopy with a finite-sized detector,[14,15] which exhibits a negative tail in the OTF when the detector size is large. Therefore, introducing optical fibers into the two-photon fluorescence microscope does not result in negative values in the OTF, thus avoiding imaging artifacts.

For finite values of A_j, the passband of the 3-D OTF in Eq. (9) is the same as that in two-photon fluorescence microscopy with the use of a finite-sized detector.[14,15] In particular, the cutoff axial and transverse spatial frequencies in Eq. (9) are 1 and 4, respectively. When either A_1 or A_2 becomes infinite, $C_1(l, s)$ or $C_2(l, s)$ approaches a delta function at the origin in spatial-frequency space and therefore the 3-D OTF reduces to

$$C(l, s) = C_2(l, s) \tag{14}$$

for A_1 approaching infinity and

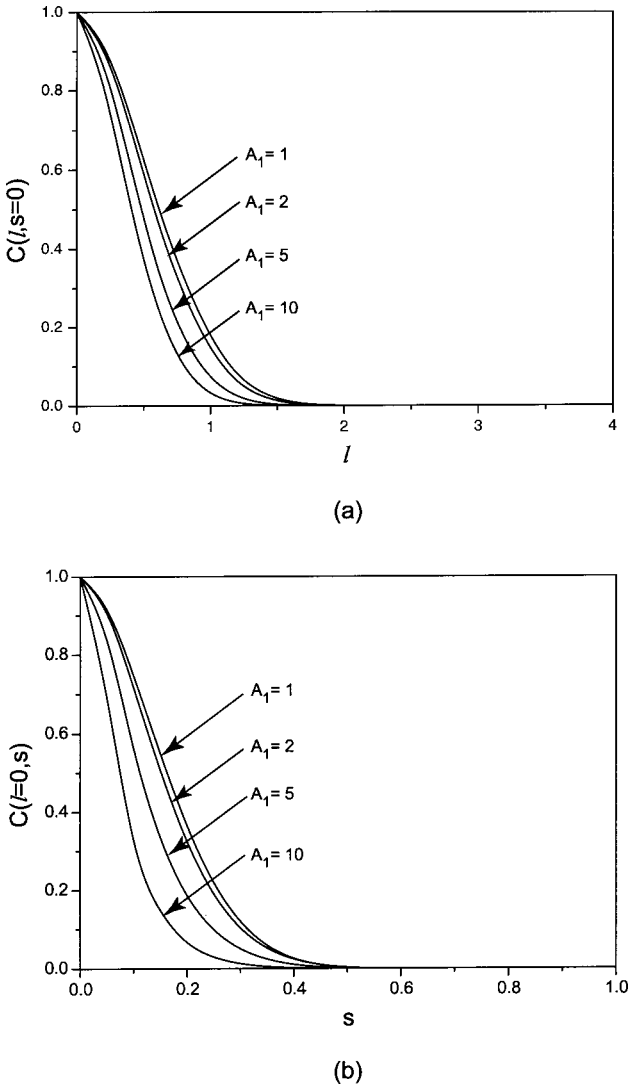

Fig. 2. (a) Transverse and (b) axial cross sections of the 3-D OTF for fiber-optical two-photon fluorescence microscopy with a large-area detector for different values of the normalized optical spot size parameter A_1 ($A_2 \rightarrow \infty$).

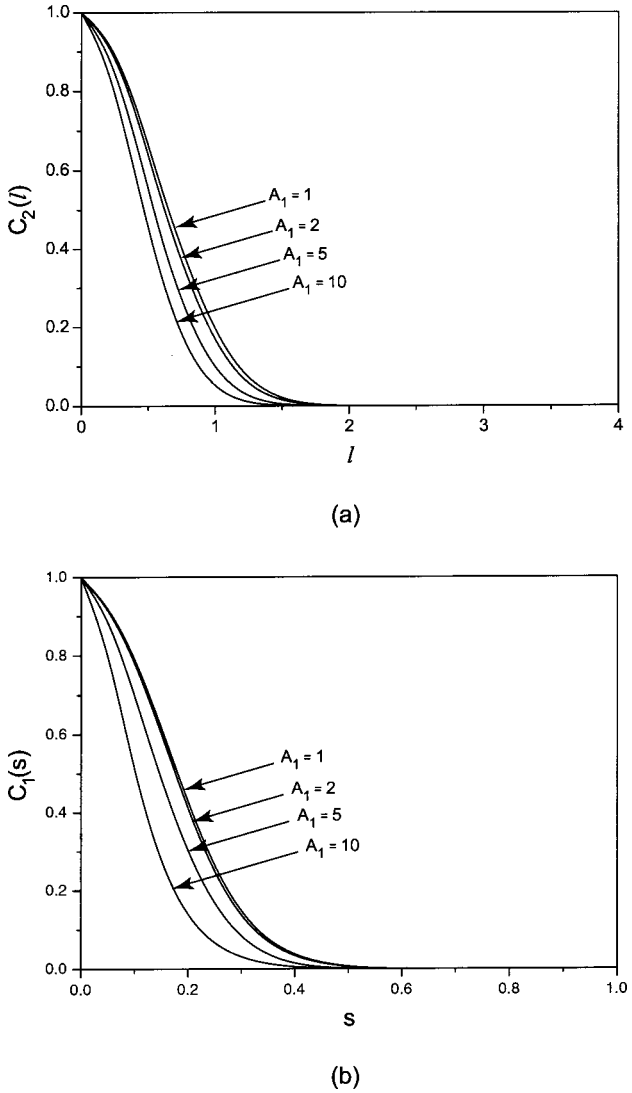

Fig. 3. (a) 2-D in-focus and (b) 1-D on-axis OTFs for fiber-optical two-photon fluorescence microscopy with a large-area detector for different values of the normalized optical spot size parameter A_1 ($A_2 \rightarrow \infty$).

$$C(l, s) = C_1(l, s) \otimes_3 C_1(l, s) \tag{15}$$

for A_2 approaching infinity. In both cases, the axial and transverse spatial frequencies are 0.5 and 2, respectively.

4. NUMERICAL RESULTS AND DISCUSSION

In this section, we investigate two particular types of fiber-optical two-photon fluorescence microscopy to understand the recent experimental results.[10,12] The first geometry involves the use of a fiber to deliver a laser beam to a conventional confocal microscope, and a large-area detector is used to collect the fluorescence signal.[10] In this case, $A_2 \rightarrow \infty$. The second system is based on an optical fiber coupler, which acts as a low-pass filter.[12] In this case, according to Eq. (12), for a fixed geometry the value of the normalized fiber parameter for collection (A_2) is approximately four times the value of the normalized fiber parameter for illumination (A_1), since the wavelength of the fluorescent light in both cases is assumed to be half that of the illumination wavelength, i.e., $\beta = 2$ in Eq. (10). This leads to numerical consideration of the case $A_2 = 4A_1$ for the second system.

For the first system ($A_2 \rightarrow \infty$), the 3-D OTF for $A_1 = 1$ and $A_1 = 10$ is shown in Fig. 1. For $A_1 = 1$, the corresponding 3-D OTF exhibits the cutoff axial and transverse spatial frequencies of 0.5 and 1, respectively, as expected. Comparing Fig. 1(a) with Fig. 1(b) reveals that when the normalized fiber spot size A_1 is small, the imaging performance of the system becomes superior. This can be seen from the fact that as A_1 increases, the responses of the 3-D OTF at high axial and transverse spatial frequencies become weaker. Therefore the cutoff spatial frequencies are effectively decreased in both the axial and transverse directions, as clearly demonstrated by the axial and transverse cross sections of the 3-D OTF shown in Fig. 2. The cross sections through the 3-D OTF at $s = 0$ and $l = 0$ correspond to imaging of a thick structure with no variation in the fluorescent strength in the axial direction and of a planar structure with no variation in the fluorescent strength in the transverse direction, respectively.[15]

The projection of the 3-D OTF in the focal plane and on the axial axis gives rise to the 2-D in-focus and one-dimensional (1-D) on-axis OTFs that describe the image

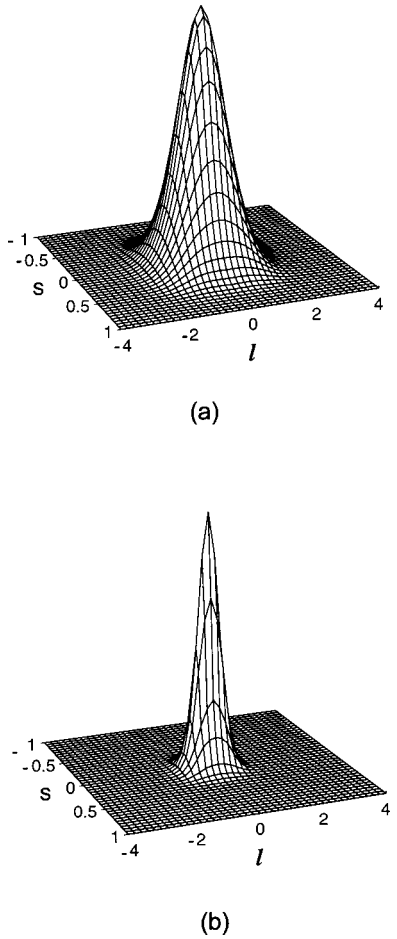

Fig. 4. 3-D OTF for fiber-optical two-photon fluorescence microscopy with an optical coupler ($A_2 = 4A_1$): (a) $A_1 = 2$, (b) $A_1 = 10$.

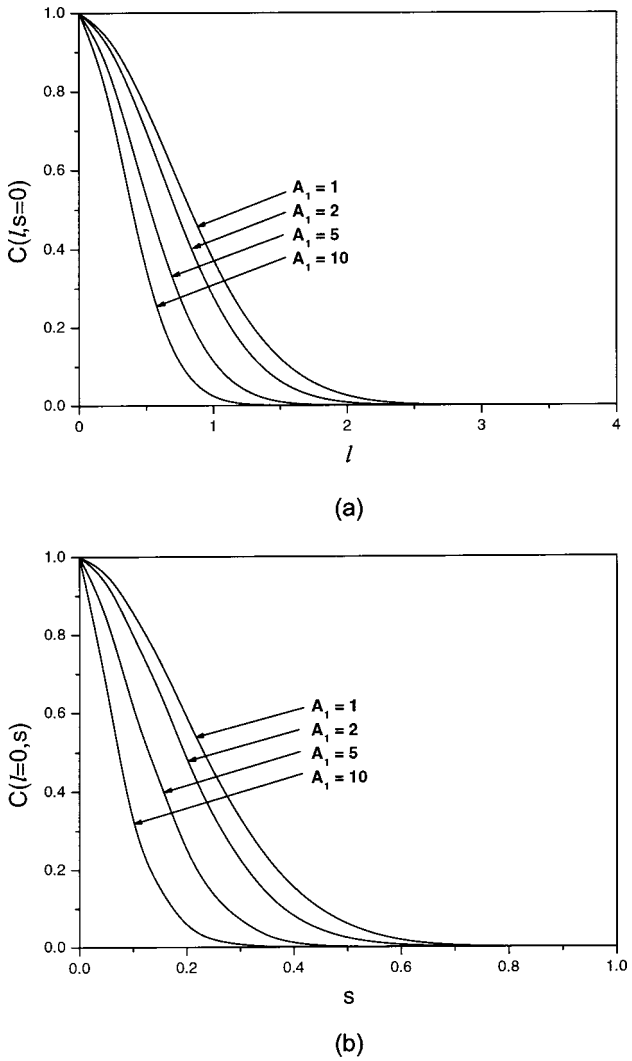

Fig. 5. (a) Transverse and (b) axial cross sections of the 3-D OTF for fiber-optical two-photon fluorescence microscopy with an optical coupler for different values of the normalized optical spot size parameter A_1 ($A_2 = 4A_1$).

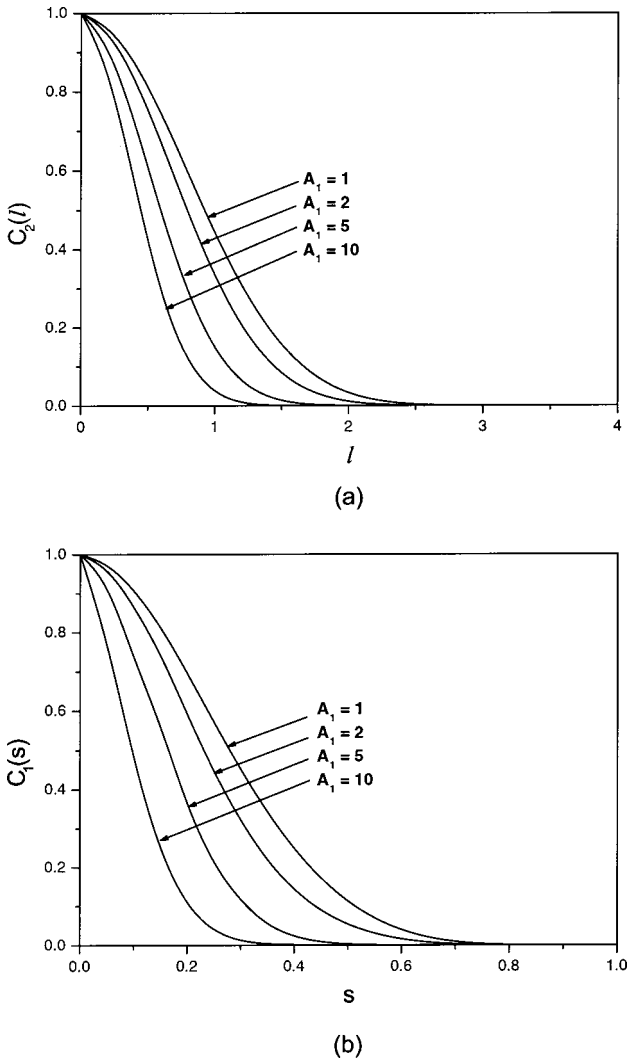

Fig. 6. (a) 2-D in-focus and (b) 1-D on-axis OTFs for fiber-optical two-photon fluorescence microscopy with an optical coupler for different values of the normalized optical spot size parameter A_1 ($A_2 = 4A_1$).

properties of a thin object in the focal plane and a line objective on the axis.[15] These two OTFs for the first two-photon system are depicted in Fig. 3. It is clear that the cutoff spatial frequencies of the 2-D in-focus and 1-D on-axis OTFs are 2 and 0.5, respectively, and that the response of these functions becomes weaker when the normalized fiber spot size is larger.

Let us turn to the second two-photon imaging system in which a fiber coupler is used.[12] Figure 4 shows the 3-D OTF in this case. Figure 4(a) is the 3-D OTF for $A_1 = 2$. A direct comparison with Fig. 1(a) shows that both the transverse and axial responses of the 3-D OTF in the former are stronger and that the cutoff spatial frequencies in both axial and transverse directions are approximately 1.7 times larger. This feature means that more information in an object can be imaged by the second two-photon system, leading to higher image resolution. However, as the value of A_1 becomes large [Fig. 4(b)], the performance of the OTF is degraded to that shown in Fig. 1(b). This is clearly demonstrated in Figs. 5 and 6, where the cross sections through the 3-D OTF at $s = 0$ and l

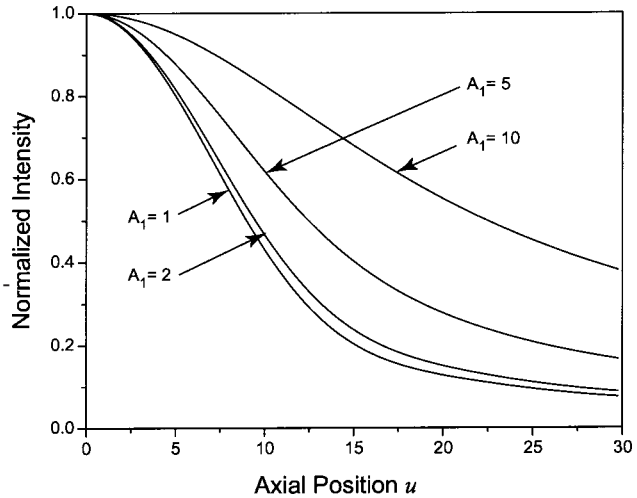

Fig. 7. Calculated axial response of a thin fluorescent sheet for fiber-optical two-photon fluorescence microscopy with a large-area detector for different values of the normalized optical spot size parameter A_1 ($A_2 \rightarrow \infty$). $u = 8\pi z \sin^2(\alpha/2)/\lambda_2$, where z is the scanning distance of the fluorescent sheet.

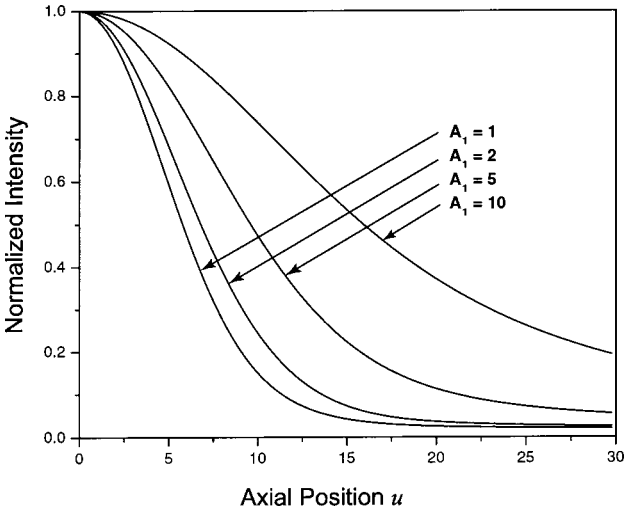

Fig. 8. Calculated axial response of a thin fluorescent sheet in fiber-optical two-photon fluorescence microscopy with an optical coupler for different values of the normalized fiber spot size parameter A_1 ($A_2 = 4A_1$). $u = 8\pi z \sin^2(\alpha/2)/\lambda_2$ where z is the scanning distance of the fluorescent sheet.

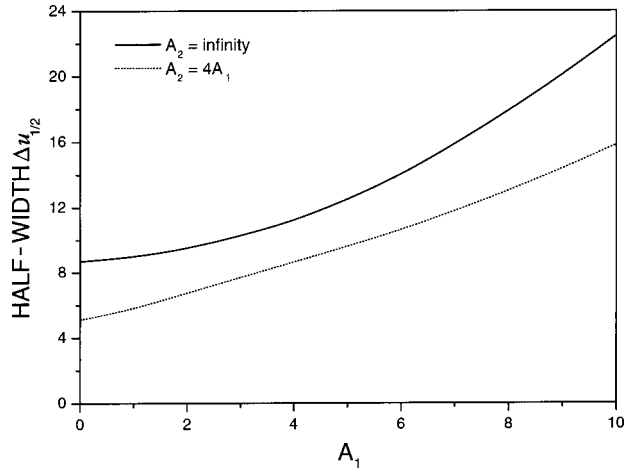

Fig. 9. Half-width at half-maximum of the axial response, $\Delta u_{1/2}$, as a function of the normalized fiber spot size parameter A_1. The solid curve is the case for fiber-optical two-photon fluorescence microscopy with a large-area detector ($A_2 \rightarrow \infty$), and the dotted curve is the case with a fiber coupler implementation ($A_2 = 4A_1$).

$= 0$ (Fig. 5) and the 2-D in-focus OTF and the 1-D on-axis OTF (Fig. 6) are shown for increasing values of A_1.

To characterize the improvement in resolution, in particular in the axial direction, we consider imaging of a thin fluorescent sheet scanning through the focus of the objective. This axial response is a measure of axial resolution or the optical sectioning property[10,12] and can be calculated by using the Fourier transform of the axial cross section of the 3-D OTF at $l = 0$.[15] Figures 7 and 8 exhibit the axial responses corresponding to the OTFs of Figs. 2(b) and 5(b) in the two considered fiber-optical two-photon imaging systems, respectively. It is clearly demonstrated that the axial resolution of both system geometries is degraded as the normalized fiber parameter A_1 is increased. This can be understood from the fact that the cutoff spatial frequencies are effectively reduced as the magnitude of the normalized fiber parameter increases.

However, for a given value of A_1, the axial response in the second imaging system is narrower than that in the first system, yielding improved axial resolution. The amount of the improvement in axial resolution can be found from Fig. 9, where the half-width at half-maximum of the axial response, $\Delta u_{1/2}$, is plotted as a function of the normalized optical parameter A_1. The solid curve corresponds to a system with a single illumination fiber and a large-area detector, while the dotted curve corresponds to an optical-fiber-coupler-based system. The improvement in axial resolution between the first and second cases is approximately 35% for $A_1 = 1$ and 30% for $A_1 = 10$, assuming a ratio of 2 for excitation wavelength to fluorescence wavelength. Under the experimental condition[10,12] of $A_1 \approx 7$, the improvement in axial resolution is approximately 25%, which is slightly less than the experimental observation[12] of 30%. This difference is caused by the fact that in this analysis the resolution improvement that arises as a consequence of nonlinear spectral broadening and blueshifting of an ultrashort-pulsed beam as it propagates within a single-mode fiber is not considered.[10] It has been shown that, as a result of these effects, an improvement in axial resolution of approximately 5%–7% is achievable,[10] which contributes to an observed resolution improvement that is greater than that in the theoretical analysis.

It should be pointed out that although the use of a fiber coupler leads to an improvement in the axial resolution and is convenient from the point of view of miniaturization, these features come at the expense of signal level. Compared with the geometry of the first system,[10] the coupler arrangement[12] is descanned, and, consequently, scattered fluorescence from deeper sections within a sample are not collected as efficiently. An experimental comparison between the two systems[10,12] in terms of the signal level reveals that for the fiber-coupler-based system the signal level is reduced by approximately 2 orders of magnitude. The significant decrease in signal level is largely attributable to a coupling efficiency of less than approximately 1% at the two-photon fluorescence wavelength of approximately 540 nm.

5. CONCLUSION

The 3-D OTF for a fiber-optical two-photon fluorescence microscope has been developed. The performance of two geometries of fiber-based imaging systems has been compared through numerical analysis. It has been shown that the transverse and axial cutoff spatial frequencies of the 3-D OTF for a single-fiber delivery system with a large-area detector are similar to those in a conventional two-photon fluorescence microscope without the use of a pinhole. However, the transverse and axial cutoff spatial frequencies of the 3-D OTF for a two-photon microscope employing a single-mode optical fiber coupler are effectively 1.7 times larger than those for the single-fiber case. As a result, the optical sectioning effect is enhanced by at least 25% when a fiber coupler is implemented, although this improvement comes at the expense of a reduction in signal level. Further, the transfer function analysis con-

firms that the 3-D OTF in fiber-optical two-photon fluorescence microscopy is always positive, which means that image artifacts that may occur in a two-photon fluorescence microscope with a finite-sized detector can be avoided.

ACKNOWLEDGMENT

The authors thank the Australian Research Council for its support.

Corresponding author Min Gu can be reached by e-mail at mgu@swin.edu.au.

REFERENCES

1. S. Kimura and T. Wilson, "Confocal scanning optical microscope using single-mode fiber for signal detection," Appl. Opt. **30**, 2143–2150 (1991).
2. J. Benschop and G. Von Rosmalen, "Confocal compact scanning optical microscope based on compact disc technology," Appl. Opt. **30**, 1179–1184 (1991).
3. M. Gu, C. J. R. Sheppard, and X. Gan, "Image formation in a fiber-optical confocal scanning microscope," J. Opt. Soc. Am. A **8**, 1755–1761 (1991).
4. A. F. Gmitro and D. Aziz, "Confocal microscopy through a fiber optic imaging bundle," Opt. Lett. **18**, 565–567 (1993).
5. T. Wilson, "Image formation in two-mode fiber-based confocal microscopes," J. Opt. Soc. Am. A **10**, 1535–1543 (1993).
6. M. Gu and C. J. R. Sheppard, "Fiber-optical confocal scanning interference microscopy," Opt. Commun. **100**, 79–86 (1993).
7. H. Zhou, C. J. R. Sheppard, and M. Gu, "A compact confocal interference microscope based on a four-port single-mode fiber coupler," Optik (Stuttgart) **103**, 45–48 (1996).
8. M. Gu and D. K. Bird, "Fiber-optical double-pass confocal microscopy," Opt. Laser Technol. **30**, 91–93 (1998).
9. P. M. Delaney, M. R. Harris, and R. G. King, "Fiber-optic laser scanning confocal microscope suitable for fluorescence imaging," Appl. Opt. **33**, 573–577 (1994).
10. D. Bird and M. Gu, "Resolution improvement in two-photon fluorescence microscopy using a single-mode fiber," Appl. Opt. **41**, 1852–1857 (2002).
11. A. Lago, A. T. Obeidat, A. E. Kaplan, J. B. Khurigan, and P. L. Shkolnikov, "Two-photon-induced fluorescence of biological markers based on optical fibers," Opt. Lett. **20**, 2054–2056 (1995).
12. D. Bird and M. Gu, "Compact two-photon fluorescence microscope using a single-mode optical fiber coupler," Opt. Lett. **27**, 1031–1033 (2002).
13. W. Denk, J. H. Strickler, and W. W. Webb, "Two-photon laser scanning fluorescence microscopy," Science **248**, 73–75 (1990).
14. M. Gu and C. J. R. Sheppard, "Effect of a finite-sized pinhole on 3D image formation in confocal two-photon fluorescence microscopy," J. Mod. Opt. **40**, 2009–2024 (1993).
15. M. Gu, *Principles of Three-Dimensional Imaging in Confocal Microscopes* (World Scientific, Singapore, 1996).
16. M. Gu, X. Gan, and C. J. R. Sheppard, "Three-dimensional coherent transfer functions in fiber-optical confocal scanning microscopes," J. Opt. Soc. Am. A **8**, 1019–1025 (1991).
17. M. Gu and C. J. R. Sheppard, "Three-dimensional optical transfer function in a fiber-optical confocal fluorescent microscope using annular lenses," J. Opt. Soc. Am. A **9**, 1991–1999 (1992).
18. S. Kimura and C. Munakata, "Calculation of three-dimensional optical transfer function for a confocal scanning fluorescent microscope," J. Opt. Soc. Am. A **6**, 1015–1019 (1989).
19. S. Kawata, R. Arimoto, and O. Nakamura, "Three-dimensional optical-transfer function analysis for laser-scan fluorescent microscope with an extended detector," J. Opt. Soc. Am. A **8**, 171–175 (1991).
20. M. Gu and C. J. R. Sheppard, "Confocal fluorescent microscopy with a finite-sized circular detector," J. Opt. Soc. Am. A **9**, 151–153 (1992).
21. M. Gu, T. Tannous, and C. J. R. Sheppard, "Three-dimensional confocal fluorescence imaging under ultrashort pulse illumination," Opt. Commun. **117**, 406–412 (1995).
22. M. Born and E. Wolf, *Principles of Optics* (Pergamon, New York, 1980).
23. B. R. Frieden, "Optical transfer of a three-dimensional object," J. Opt. Soc. Am. **57**, 56–66 (1967).
24. A. W. Snyder and J. D. Love, *Optical Waveguide Theory* (Chapman & Hall, London, 1983).
25. I. S. Gradstein and I. M. Ryshik, *Tables of Series, Products and Integrals* (Deutscher, Verlag, Frankfurt, 1981).